of other species. The short answer is 'yes', and is best illustrated by a return to an earlier example – interactions between species on rocky shores of islands on the west coast of South Africa (**Figure 3**). In its undisturbed state, each of the key interactions in this ecosystem is buffered in some way. Limpets are consumed by oystercatchers, but some escape by growing too large to be eaten, aided by the high primary production. Limpets and other invertebrates graze on algae, but their effects are muted by predation on them and by the enhancement of algal growth by guano. Waders eat small seaweed-associated invertebrates, but emigrate in winter.

For several reasons, human impacts are not constrained in these subtle ways. First, human populations do not depend on rocky shores in any manner limiting their own numbers. They can harvest these resources to extinction with impunity. Second, modern human effects are too recent a phenomenon for the impacted species to have evolved defenses. Thirdly, humans are supreme generalists. Simultaneously, they can act as predators, competitors, amensal disturbers of the environment, and 'commensal' introducers of alien species. Fourthly, money, not returns of energy, determines profitability. Fifthly, long-range transport means that local needs no longer limit supply and demand. Sixthly, technology denies resources any refuge.

Thus, humans supersede the ecological and evolutionary rules under which natural systems operate; and only human-imposed rules and constraints can replace them in meeting our self-proclaimed goals of sustainable use and maintenance of biodiversity.

See also

Beaches, Physical Processes Affecting. Coastal Circulation Models. Coastal Trapped Waves. Eutrophication. Exotic Species, Introduction of. Internal Tides. Intertidal Fishes. Macrobenthos. Seabird Conservation. Seabirds and Fisheries Interactions. Tides. Upwelling Ecosystems. Waves on Beaches.

Further Reading

Branch GM and Griffiths CL (1988) The Benguela ecosystem Part V. The coastal zone. *Oceanography and Marine Biology Annual Review* 26: 395–486.

Castilla JC (1999) Coastal marine communities: trends and perspectives from human-exclusion experiments. *Trends in Ecology and Evolution* 14: 280–283.

Connell JH (1975) Some mechanisms producing structure in natural communities: a model and evidence from field experiments. In: Cody ML and Diamond JM (eds) *Ecology and Evolution of Communities*, pp. 460–490. Cambridge, MA: Belknap Press.

Denny MW (1988) *Biology and the Mechanics of the Wave-swept Environment*. Princeton, NJ: Princeton University Press.

Hawkins SJ and Hartnoll RG (1983) Grazing of intertidal algae by marine invertebrates. *Oceanography and Marine Biology Annual Review* 21: 195–282.

Menge BA and Branch GM (2001) Rocky intertidal communities. In: Bertness MD, Gaines SL and Hay ME (eds) *Marine Community Ecology*. Sunderland: Sinauer Associates.

Moore PG and Seed R (eds) (1985) *The Ecology of Rocky Coasts*. London: Hodder and Stoughton.

Newell RC (1979) *Biology of Intertidal Animals*. Faversham, Kent: Marine Ecological Surveys.

Paine RT (1994) *Marine Rocky Shores and Community Ecology: An Experimentalist's Perspective*. Oldendorf: Ecology Institute.

Siegfried WR (ed.) (1994) *Rocky Shores: Exploitation in Chile and South Africa*. Berlin: Springer-Verlag.

Underwood AJ (1997) *Experiments in Ecology: their Logical Design and Interpretation Using Analysis of Variance*. Cambridge: Cambridge University Press.

ROSSBY WAVES

P. D. Killworth, Southampton Oceanography Centre, Southampton, UK

doi:10.1006/rwos.2001.0120

Introduction: What Are Rossby Waves?

Among the many wave motions that occur in the ocean, Rossby (or planetary) waves play one of the most important roles. They are largely responsible for determining the ocean's response to atmospheric and other climate changes; their energy dominates the ocean's energy spectrum at long timescales; they are responsible for setting up and maintaining the intense oceanic western boundary currents, and can be generated by those currents; they affect ocean color and biological interactions near the surface; and they moderate the ocean's behavior to decadal features such as El Niño and the North Atlantic Oscillation. The waves have a strong westward

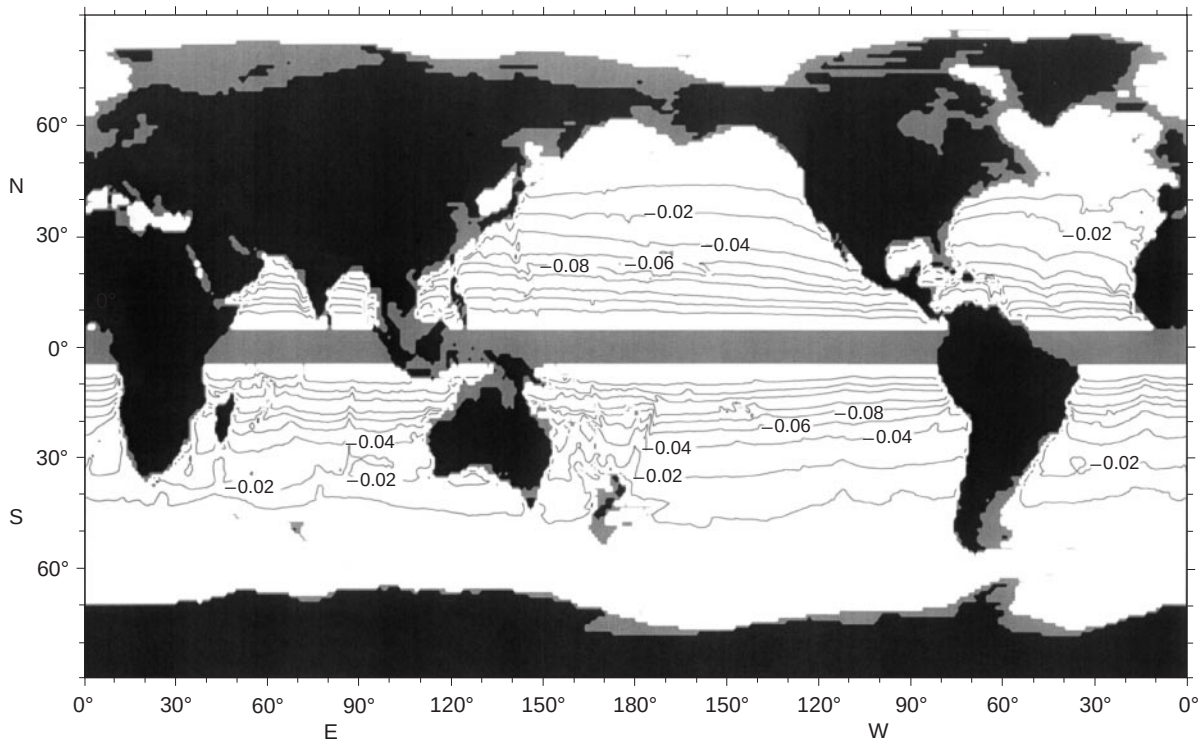

Figure 1 Contours of the speed of the fastest long baroclinic Rossby wave ($m\,s^{-1}$). Contour intervals are nonuniform: 0.3, 0.2, 0.15, 0.1, 0.08, 0.06, 0.04, 0.02, 0.01 $m\,s^{-1}$. Negative signs mean speed is westward. Values are masked within 5° of the equator where other theory holds, and for depths of less than 1000 m.

component in their phase speed (though short waves can propagate their energy eastward). There are two types of Rossby wave, as with many oceanic waves. The first is barotropic (independent of depth), which propagates rapidly (typically at 50 $m\,s^{-1}$), has variable space and time scales, and can cross an ocean basin in a few days. The second type of Rossby wave is baroclinic (varying with depth) and propagates fairly slowly (a few centimeters per second), has a long space scale (hundreds of kilometers), has a long period (of order a year), and takes a decade or more to cross an ocean basin westward. There is a countable infinity of baroclinic modes, but just one barotropic mode. Similar waves exist in the atmosphere, and are known to be responsible for most of the low-frequency variability observed there.

Figure 1 shows contours of the speed of the fastest propagating depth-varying Rossby wave within the ocean. This speed, as we shall see, increases dramatically near the equator, and decreases to become very slow at high latitudes.

All waves exist and propagate because of waveguides. Rossby waves owe their existence to an east–west waveguide that is present because the Coriolis parameter increases northward. In the simplest case of depth-independent two-dimensional flow (**Figure 2**), wave propagation occurs because of conservation of absolute vorticity of a fluid particle. (Absolute vorticity is the sum of the rotational, or relative, vorticity due to water motions plus the intrinsic, or planetary, vorticity due to the background earth rotation.) Imagine a line of particles oriented east–west (**Figure 2A**). These particles have no relative vorticity and no current shear. Now suppose the line is perturbed north–south in some manner (**Figure 2B**). The particles moved northward increase their intrinsic vorticity. To conserve their absolute vorticity, they must acquire negative rotational vorticity. The particles moved southward similarly acquire positive rotational vorticity. The rotational motions induced by these vorticity changes are shown in **Figure 2C**, and their effect on the particles in **Figure 2D**. The net effect is to move the original disturbed pattern of particle positions (B) westward.

In the more usual case of depth-varying flow, consider the ocean stratification as comprising a single layer of uniform depth H. When particles are displaced, they conserve their (potential) vorticity, which is now given for long length scales by f/H, where f is the Coriolis vector (the vorticity argument above continues to hold for short length scales). It is the variation of this quantity north–south that again induces a westward wave

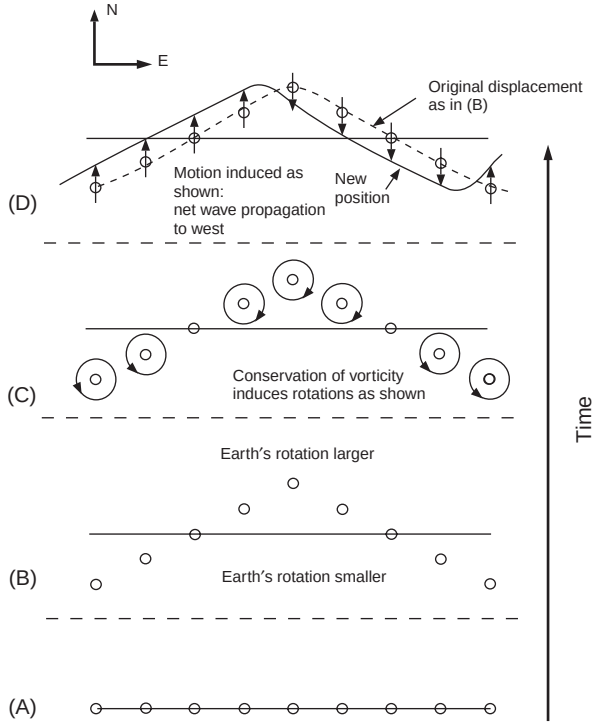

Figure 2 Schematic of depth-independent Rossby wave transmission; time reads up the diagram. An east–west line of particles (A) is displaced (B) and gathers vorticity owing to changes in the background Earth's rotation (C). This vorticity induces flow changes (D) that act to move the displacement pattern westward.

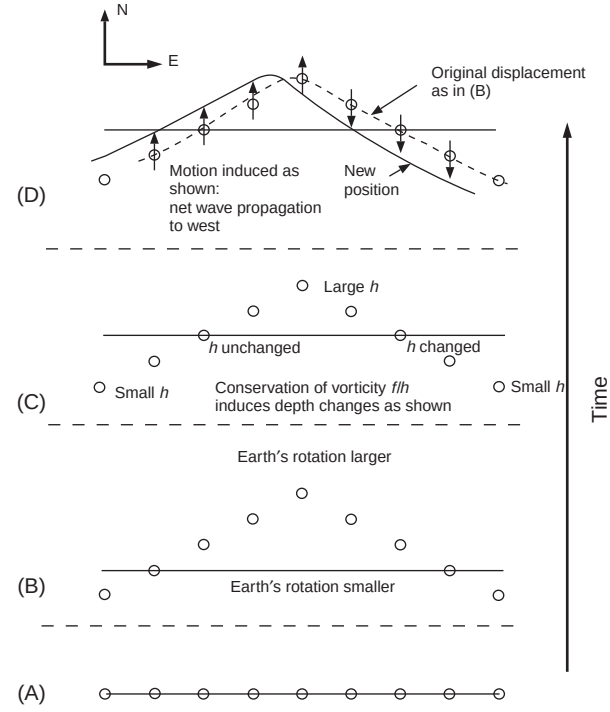

Figure 3 As Figure 2, but for a fluid layer. As the layer is displaced (B), it changes its depth (C) to conserve potential vorticity. These depth changes induce geostrophic flows (D) that act to move the displacement pattern westward.

propagation. Particles displaced northward (**Figures 3A** and **B**) increase f and so increase H to compensate; particles moving southward decrease H. Thus the particle motions in **Figure 3C** give depth – and hence pressure – changes that lead to geostrophic flows (**Figure 3D**) that have similar effects on the displacements, moving the pattern westward. These schematic arguments also hold, with some modifications, near the equator.

For most practical purposes of measurement, Rossby waves propagate as a series of low and high pressures, which are constant normal to the direction of wave phase propagation. The resulting geostrophic flow is alternately in one direction and then in the opposite, perpendicular to the propagation direction. **Figure 4** shows an example of this.

The generation mechanisms for Rossby waves are unclear, though some form of surface forcing must be involved to induce changes in the upper ocean structure which can then propagate as waves. Thus, direct forcing by wind stress and to a lesser extent, by buoyancy forcing will both generate Rossby waves. Free waves must still be forced somewhere, and possible candidates include upwelling and downwelling on the eastern boundary induced by alongshore wind stress and topographic wave shedding over ocean ridges.

Observations of Rossby Waves

Rossby waves have been well observed in the atmosphere for decades. The large scale of oceanic Rossby waves necessitates an array of observations

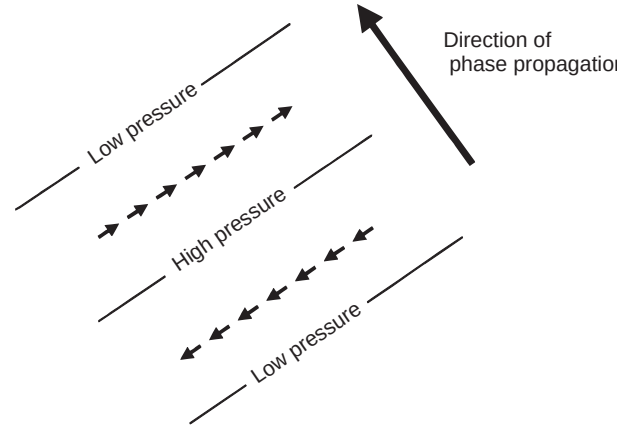

Figure 4 Schematic of long Rossby wave motions, which lie predominantly normal to the direction of phase propagation.

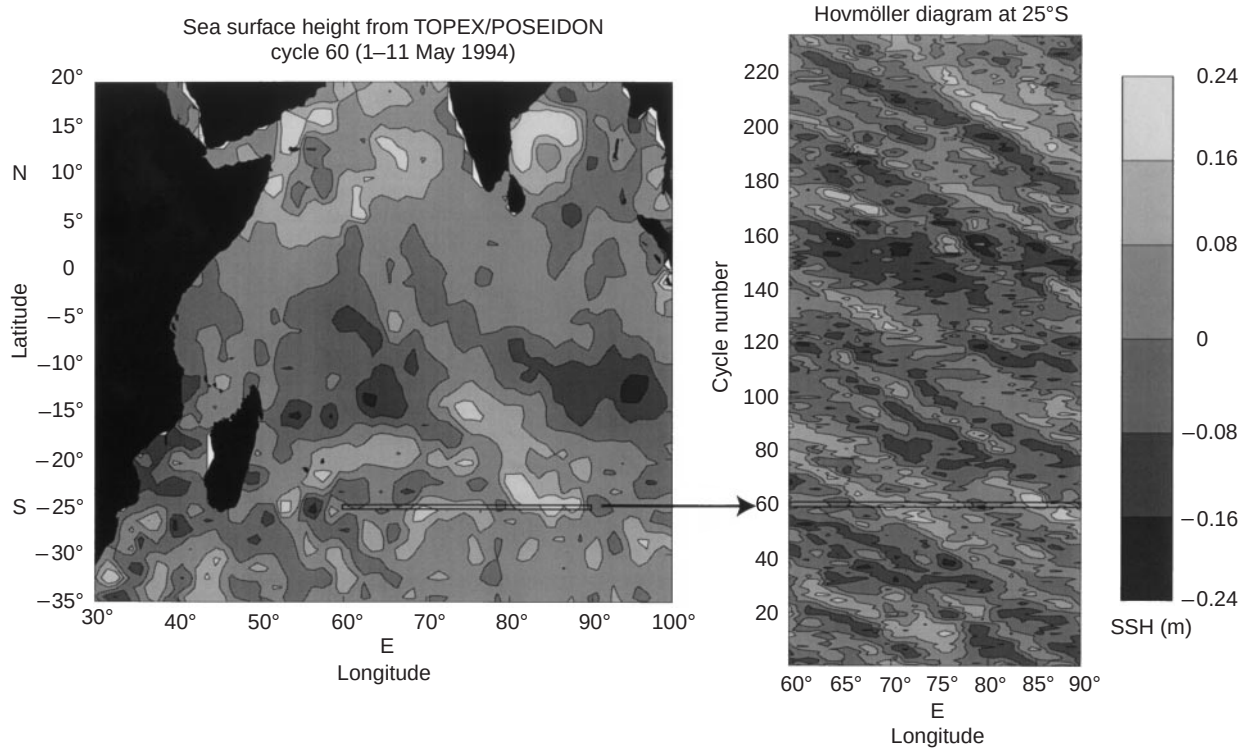

Figure 5 Hovmöller (or time–longitude) diagram, and its method of generation, for the South Indian Ocean. Snapshots of sea surface height (SSH) are taken along a given latitude at each satellite cycle (left-hand side of diagram) and assembled in sequence with time running upward (right-hand side of diagram). The signals of westward propagation then show clearly as bands tilted from upper left to lower right. One cycle is about 10 days. Note the amplitudes, typically about 10 cm and speed of waves, about 0.06 m s^{-1}.

spanning a noticeable fraction of an ocean basin to distinguish phase variations, and the data obtained from cruises and ships of opportunity have been inadequate for the task, despite some valiant efforts. Rossby waves were, therefore, remarkably difficult to observe in the ocean until recently. (Observing barotropic Rossby waves is likely to continue to be difficult: their high speed makes the design of an observation network almost impossible.) Thus the theory of Rossby waves, discussed below, considerably predates their observation.

The launch of altimetric satellites changed all this dramatically. The barotropic Rossby waves remained essentially unobservable by satellites (the phases move so rapidly that they become indistinguishable between satellite passes). However, altimeter coverage proved ideal for the detection of surface signatures of baroclinic waves, which possessed surface height variations of a few centimeters and so were, at least for the TOPEX/Poseidon instrument, observable to the accuracy of the altimeter.

Satellite altimeters, to date, can only provide relative measures of sea surface height; in other words, they can report the variation of height accurately, but not the absolute value. For the purposes of observing wave propagation, this limitation presents no difficulties. Nonetheless, the ocean surface variation is made up of a superimposition of many different waves, direct responses to local forcing, and so on, so that the detection of Rossby waves still required massaging of the data.

The simplest approach used is to construct a time–space, or Hovmöller, diagram (**Figure 5**). A specific geographical line along which wave propagation is to be studied is chosen, typically a line of constant latitude. At successive times, determined by the repeat pattern of the satellite, the surface height – usually measured relative to some long-term average at each location so as to remove as much bias as possible – is plotted as a function of distance along the chosen line. These plots are then stacked perpendicular to each other, at separations proportional to the time interval. Wave propagation will then appear as contour lines across the diagram; the slope of these lines is a direct measure of the speed of the wave. Waves propagating at constant speed show up as lines of constant slope; those whose speed varies along the line will show a slope variation. In some cases more than one wave can

be inferred, suggesting that various vertical modes are present simultaneously. There are hints that waves are sometimes generated near midocean ridges, though the reasons are as yet unclear. Certainly wavelike features can be identified in many parts of the ocean by this approach.

The Hovmöller diagram approach as in **Figure 5** is biased toward the direction of the chosen line (in this case toward east–west propagation). Here waves can be seen propagating 30° in longitude in about 60 cycles, with a cycle time of 10 days, this gives a speed of $0.06\,\mathrm{m\,s^{-1}}$. Lines can be, and have been, oriented at other angles, but obviously a more systematic approach is necessary to locate the preferred orientation of the waves. Various methods have been used (e.g., Fourier transforms), with a popular approach being the Radon transform. This can be thought of as a simultaneous examination of Hovmöller diagrams at all possible angles, seeking for the orientation that gives the most energetic signal. So far, the preferred orientation for waves has been within a few degrees of westward, despite the fact that north–south propagation remains perfectly possible in theory. The reason remains unknown.

Detection is made more uncertain by the difficulty of disentangling other possible mechanisms that might have produced the given pattern. For example, a westward propagating eddy would appear as a wave on a Hovmöller diagram, while a propagating disturbance on a western boundary layer could appear as an eastward-oriented wave.

Recent increases in accuracy of other satellite instrumentation has meant that these too can be used to detect Rossby waves (and, more generally, large-scale anomaly propagation). Sea surface temperature measurements are a case in point. Their signal is dominated by the seasonal cycle. This can be removed in various ways (e.g., by removing the cycle explicitly at each location, or by taking the east–west derivative of the data at each point). The resulting signal also shows westward-propagating modes at similar, but not identical, speeds to the altimeter in most cases. This has been interpreted as the simultaneous presence of wave modes with different vertical structures (and so with different speeds). In the altimeter signal, one wave appears dominant; in the surface temperature signal, another mode is dominant. This is confirmed by theory, which shows that the relation between surface height and temperature variability depends strongly on the vertical structure of the wave, so that each wave could appear dominant when observed by one of the instruments.

Ocean color passive microwave instruments are now also used to elucidate large-scale wave propagation.

Theory of Rossby Waves

Theoretical predictions of Rossby waves have existed since the 1930s, and have long been known to give good predictions for atmospheric motions. The theory involves taking the three-dimensional problem and splitting it into two subproblems. The first involves the horizontal and time (as in the schematics above) and the second involves only the vertical structure. The latter is known as 'normal mode theory.' The idea is to find vertical structures that are maintained as the wave propagates, leaving the actual propagation behavior to be described by the pseudo-horizontal problem.

Horizontal Variation

It is logical to begin with the horizontal problem, for small motions in an ocean of uniform depth H, with a perturbation h. (An effective depth H will be determined later.) The momentum equations in the east (x) and north (y) directions for the velocity components (u, v, respectively) are

$$u_t - fv = -gh_x \qquad [1]$$

$$v_t + fu = -gh_y \qquad [2]$$

since the dynamic pressure (p/ρ_0, where p is pressure and ρ_0 the mean density of sea water) is given by gh. Here h_x means $\partial h/\partial x$. Conservation of mass gives

$$h_t + H(u_x + v_y) = 0 \qquad [3]$$

The dispersion relation for wave motions satisfying these equations involves a little work, since the coefficients possess y-variation due to the terms in f. To a good degree of approximation, if the waves are slow (formally, $\partial/\partial t$ is assumed small compared with f), the velocity components are

$$u \approx \frac{gh_y}{f} - \frac{gh_{xt}}{f^2} \qquad [4]$$

$$v \approx \frac{gh_x}{f} - \frac{gh_{yt}}{f^2} \qquad [5]$$

and substitution of these into mass conservation gives a single equation for h:

$$\frac{\partial}{\partial t}(h - a^2\nabla^2 h) - \frac{\beta C^2}{f^2}h_x \approx 0 \qquad [6]$$

where $\nabla^2 = (\partial^2/\partial x^2) + (\partial^2/\partial y^2)$ and various small terms have been neglected, and

$$C^2 = gH \qquad [7]$$

is the speed of long surface waves and

$$a = C/f \qquad [8]$$

is the 'deformation radius,' or 'Rossby radius,' the natural length scale for the problem. Here β represents df/dy, the northward gradient of the Coriolis parameter. Equation [6] represents conservation of vorticity of the fluid column. Although its coefficients depend on latitude, because no more differentiation is required, it is traditional to 'freeze' the coefficients and treat f and β as if they are constant. We then pose

$$h \propto \exp \mathrm{i}(kx + ly - \omega t) \qquad [9]$$

which gives the dispersion relation connecting frequency ω with wavenumbers k, l as

$$\omega = -\beta a \frac{ak}{1 + (aK)^2} \qquad [10]$$

where

$$K^2 = k^2 + l^2 \qquad [11]$$

is the modulus of the wavenumber. Equation [10] has been written in a manner that emphasizes the importance of the size of the wavenumber in units of inverse deformation radius. From the dispersion relation all details of wave propagation may be determined.

To start with, [10] does not permit waves of all frequencies; there is a cutoff frequency of $|\beta a|^2$, above which Rossby waves may not propagate. Since a varies inversely with Coriolis parameter, this frequency becomes smaller as the poles are approached. (Baroclinic waves at the annual cycle can only exist for latitudes less than about 40–45°, for example.)

The phase velocity (c_x, c_y) is formally given by

$$c_x = \frac{\omega k}{K^2} = -\beta a^2 \frac{(ak)^2}{(aK)^2[1 + (aK)^2]} \qquad [12]$$

$$c_y = \frac{\omega l}{K^2} = -\beta a^2 \frac{(ak)(al)}{(aK)^2[1 + (aK)^2]} \qquad [13]$$

although these are not the propagation speeds of points of constant phase in the x and y directions, which are given by ω/k and ω/l, respectively. The first of these shows that waves propagate with crests moving westward (i.e., c_x is negative), with a maximum speed βa^2, when k and l are small (long waves). Since a varies inversely with Coriolis parameter, this speed will be a strong function of latitude, becoming infinite at the equator, where this midlatitude theory breaks down. The north–south phase velocity can take various values depending on the orientation of the wave crests.

The group velocity (c_{gx}, c_{gy}), i.e., the velocity at which the wave energy propagates, is given by

$$c_{gx} = \frac{\partial \omega}{\partial k} = -\beta a^2 \frac{1 + [(al)^2 - (ak)^2]}{[1 + (aK)^2]^2} \qquad [14]$$

$$c_{gy} = \frac{\partial \omega}{\partial l} = 2\beta a^2 \frac{(ak)(al)}{[1 + (aK)^2]^2} \qquad [15]$$

In general the group velocity is not the same as the phase velocity, so that Rossby waves are dispersive. If ak is sufficiently large (i.e., the waves are sufficiently short in the east–west direction), eqn [14] shows that c_{gx} can be positive: while crests move west, the wave energy moves east. The simplest case to discuss is when al is small, so that the waves are long in the north–south direction. Then the dispersion relation becomes

$$\omega = -\beta a \frac{ak}{1 + (ak)^2}; \qquad c_x = -\beta a^2 \frac{1}{1 + (ak)^2};$$

$$c_{gx} = -\beta a^2 \frac{1 - (ak)^2}{[1 + (ak)^2]^2} \qquad [16]$$

which is shown in **Figure 6**. This shows the following.

- Long waves ($ak \ll 1$) have the same phase and group velocity, $-\beta a^2 = -\beta C^2/f^2$, and so are nondispersive.
- Zero group velocity occurs when $ka = -1$.
- There is a maximum eastward group velocity of one-eighth the fastest westward group velocity.

Vertical Variation

We now return to the vertical structure of the waves. The idea is to seek a situation in which the waves may propagate without changing that structure. Write

$$\left(u, v, \frac{p}{\rho_0}\right) = (\tilde{u}, \tilde{v}, g\tilde{h})(x, y, t) \cdot \hat{u}(z) \qquad [17]$$

$$w = \tilde{w}(x, y, t) \cdot \hat{w}(z). \qquad [18]$$

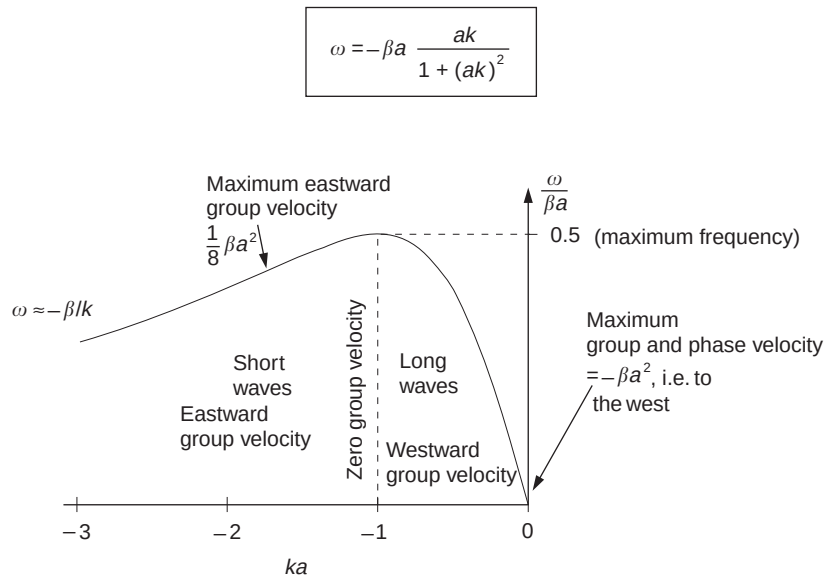

Figure 6 Dispersion diagram for Rossby waves that are long north–south, showing frequency ω as a function of east–west wavenumber k (assumed negative).

Substitution into the two horizontal momentum and the divergence, buoyancy, and hydrostatic equations, linearized about a basic state of stratification $\bar{\rho}(z)$, where $N^2(z) = -g\bar{\rho}_z/\rho_0$ is the buoyancy frequency, gives respectively

$$(\tilde{u}_t - f\tilde{v})\hat{u} = -g\tilde{h}_x\hat{u} \qquad [19]$$

$$(\tilde{v}_t + f\tilde{u})\hat{u} = -g\tilde{h}_y\hat{u} \qquad [20]$$

$$(\tilde{u}_x + \tilde{v}_y)\hat{u} + \tilde{w}\hat{w}_z = 0 \qquad [21]$$

$$-\frac{g\rho_t}{\rho_0} + \tilde{w}N^2\hat{w} = 0 \qquad [22]$$

$$-\frac{g\rho}{\rho_0} = g\tilde{h}\hat{u}_z \qquad [23]$$

(Note that the density ρ has not had a vertical structure defined but that its vertical structure is like $N^2\hat{w}(z)$). Eqs [19] and [20] already permit the cancellation of the common factor $\hat{u}(z)$ as required. Equation [21] will also permit cancellation of $\hat{u}(z)$ provided that we choose

$$\hat{w}(z) = \hat{u}_z(z) \qquad [24]$$

Finally, combination of eqns [22] and [23] can only permit cancellation of the vertical structure if

$$\hat{u}_z(z) \propto N^2\hat{w} \qquad \text{or} \qquad \hat{w}_{zz} + \frac{N^2}{C^2}\hat{w} = 0 \qquad [25]$$

Here C, with dimension of velocity, is an unknown constant of proportionality. It is given as an eigenvalue by solving eqn [25] with suitable boundary conditions at surface and floor.

There are a countable infinity of solutions, or normal modes. The zeroth (using a traditional numbering) is the barotropic mode, in which $\hat{u}$ is approximately independent of depth and $\hat{w}$ is linear with depth; C is given to an excellent degree of approximation by $C^2 = gH$, where H is the fluid depth. This gives values for C of around $200\,\mathrm{m\,s^{-1}}$ in ocean depths of 4000 m. This is just the long-wave speed of an unstratified fluid. The remaining solutions, called baroclinic, have much smaller eigenvalues C, and for these modes, to a good approximation, $\hat{w}$ vanishes at surface and floor. The nth vertical mode has $n-1$ zeros of $\hat{w}$ and n zeros of $\hat{u}$ in the fluid column, so that high modes oscillate strongly in the vertical. For various reasons, many not well understood, high modes are rarely found in observations. Typical values of C are $2–3\,\mathrm{m\,s^{-1}}$ for the first mode, and steadily slower for high modes. **Figure 7** shows the vertical structure of $\hat{w}$ and $\hat{u}$ for the first two baroclinic modes, for the stratification (N) shown, which is an average over the major ocean basins.

Substitution back into the remaining (horizontal) part of the system gives for each normal mode in turn,

$$\tilde{u}_t - f\tilde{v} = -g\tilde{h}_x \qquad [26]$$

$$\tilde{v}_t + f\tilde{u} = -g\tilde{h}_y \qquad [27]$$

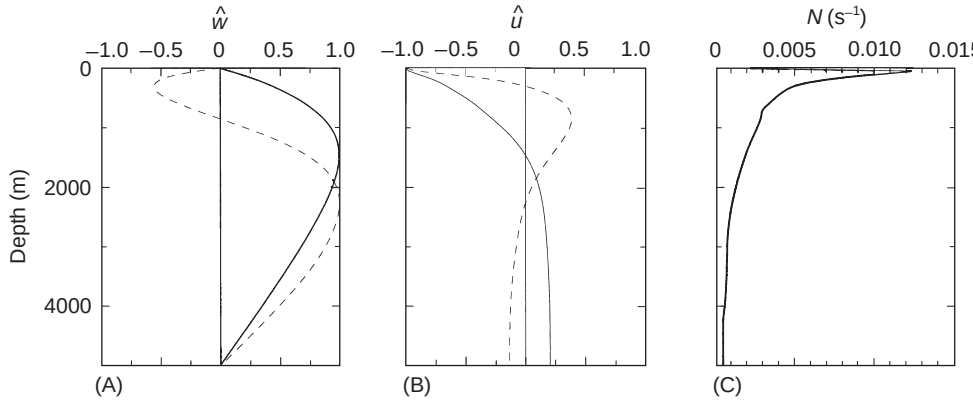

Figure 7 Vertical structure of the first two baroclinic modes, for the mean stratification of the major ocean basins: (A) $\hat{w}$; (B) $\hat{u}$; (C) N. Each mode is scaled to a maximum of unity.

$$g\tilde{h}_t + C^2(\tilde{u}_x + \tilde{v}_y) = 0 \qquad [28]$$

If we define an effective depth H by

$$H = C^2/g \qquad [29]$$

then the system of eqns [26] and [28] reduces to [1] to [3], as required, though with H taking a different meaning. Thus each vertical mode has a separate horizontal behavior, characteristic speeds, and so on.

The fastest westward phase speed (i.e., for long waves), $-\beta a^2 = -\beta C^2/f^2$, for mode 1, the fastest baroclinic mode, is shown in **Figure 1**.

Time Variation: Ocean Spinup

The theory above is derived for free waves. When the waves are forced, the approach is to express the forcing as a sum of vertical normal modes in the same way, with coefficients varying with (x, y and t), and add the forcing on the right-hand-sides of eqns [26] to [28]. The simplest such problem is the response of an ocean to a wind that is suddenly turned on; for simplicity the wind does not vary east–west.

Several things happen immediately, indicated in the Hovmöller diagram in **Figure 8**. In the ocean interior, where no waves have yet reached, the ocean responds linearly in time to the local forcing. Near the eastern boundary, a Rossby wave is initiated, carrying with it information that the ocean has an eastern boundary. This moves westward at the long-wave speed $-\beta a^2$. Behind it, the ocean becomes steady, in Sverdrup balance with the forcing. Near the western boundary, short waves, moving at speed $\beta a^2/8$, move eastward, conveying information about the western boundary to the fluid interior. (The solution left behind by these waves is complicated, and is heavily affected by any dissipative terms present.) Eventually the two wavefronts meet, giving a long-term solution with Sverdrup balance over most of the ocean, and a time-varying area near the western boundary that takes the form of an effective western boundary current.

Comparison with Observations

The satellite observations of Rossby waves discussed above showed that Rossby waves were found in many areas of the subequatorial and subpolar

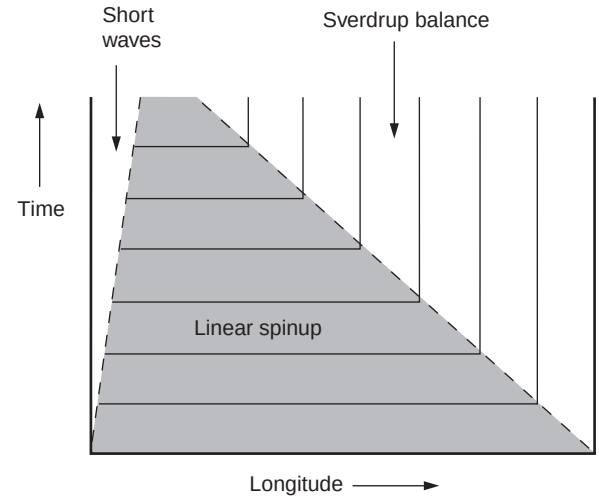

Figure 8 Schematic Hovmöller diagram showing the ocean's response to an applied steady wind stress. Long Rossby waves from the east and short, slower Rossby waves from the west move from their respective boundaries. Where they have not yet reached there is a linear spinup. After the wavefront has passed, a Sverdrup interior and a time-varying western boundary current remain.

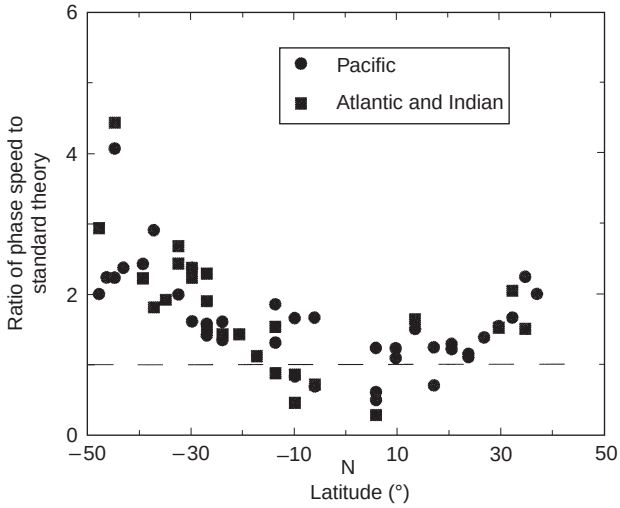

Figure 9 Ratio of observed Rossby wave speeds to linear theoretical predictions, as a function of latitude. Data from different ocean basins are indicated. The uncertainty in the ratio values is far less than the variation with latitude.

oceans. Their westward speeds were estimated using the Hovmöller diagram, or other approaches, and compared with the theory above (as indicated in **Figure 1**). The findings fall into three latitudinal bands (**Figure 9**). First, near the equator, observed wave speeds were usually somewhat less than predicted by theory. However, some of this area would be affected by equatorial wave theory, so making comparison difficult. Second, around latitudes of 10° to 20°, linear theory has succeeded admirably in estimating wave speeds. Third, for latitudes poleward of 20°, there appears to be a steady increase in the discrepancy between theory and observations, with theoretical speeds becoming as much as 2–3 times slower than observed speeds at high latitudes. (Some debate remains as to the magnitude of this shortfall, which depends to some extent on the longitude bands chosen for comparison. But the shortfall at high latitudes does seem to be unequivocal.) In areas such as the Antarctic Circumpolar Current (ACC), there is evidence of eastward propagation of Rossby waves. This is almost certainly caused by a combination of two factors: the natural speed of Rossby waves is very small at high latitudes, and the ACC is one of the few currents where the barotropic mean flow is large and eastward. Thus, the waves are simply swept eastward by the mean flow in a Doppler shift process.

Improvements to Theory

Several suggestions have been made to explain the discrepancies, which assume either that the interpretation of the data is incorrect (i.e., that linear theory is in fact correct), or that some aspect of linear theory must be modified. The answer probably lies in a combination of these.

If the waves are forced by a wind which has (say) an annual cycle, then the ocean responds with a combination of free propagating waves (e.g., as $\sin(kx - \omega t)$) and a forced response (e.g., as $\sin \omega t$). The sum of these two possesses a term in $\sin(kx - 2\omega t)$, and it could be this term that apparently yields wave propagation at twice the predicted value. However, this term occurs multiplied by $\sin kx$, and so the waves disappear at regular intervals east–west, which is not generally observed; in addition, Fourier and other methods of signal processing would show the two linear responses and not generate an erroneous doubling of the speed.

It is thus probable that some aspect of flat-bottom, dissipation-free linear theory has broken down. A prime candidate during the last 20 years has been that of varying ocean topography, which can generate a waveguide and permit the propagation of 'topographic Rossby waves' in which the bottom slope plays a role similar to that of the variations of Coriolis parameter. The resulting waves are frequently, but not always, trapped near the bottom; these waves can be faster or slower than their flat bottom relatives. Whether a topography that both rises and falls (e.g., over a midocean ridge) would generate any net speed increase remains unclear.

Active research is examining various options.

- If the waves are dissipative (either directly, or indirectly by heat losses at the surface), then the generation of a decay scale can induce an apparently different phase speed. This mechanism is particularly effective near an eastern boundary; if it is too successful, the dissipation stops the wave propagation completely.
- If the waves are of large enough amplitude, several things can happen. Pairs of waves can interact. Single large waves (sometimes known as 'solitons') can self-advect, at speeds that may differ from linear wave theory. Both these effects are beyond the scope of this article. Large waves can modify the ocean background stratification and increase their speed. However, the ubiquity of faster propagation at mid to high latitude would argue for almost permanent changes to the background stratification, which are not observed.
- The effects of ocean topography are being reexamined, with emphasis on the propagation of waves over a slowly varying floor (and concomitant normal mode change during the

propagation). The results are as yet incomplete, but it looks as though the suggestion above that topography oriented in a variety of directions cannot yield a net speed increase continues to hold.

- The mid-latitude ocean is known to possess teleconnections with the equatorial ocean, so that there may be anomalous responses at mid latitude related to the faster-travelling equatorial systems. It is hard to see how this effect could propagate to higher latitudes, however, where there would be a severe mismatch in speeds.
- Finally, the background ocean is not at rest. This has three possible effects. First, a strong enough barotropic flow could simply sweep the waves westward with the speed of the flow. However, we do not believe that depth-averaged midocean flows are even one-twentieth of the speed necessary to achieve this; so the barotropic flow can be discounted. Second, mean flow could change the normal mode calculation in the vertical. However, oceanic motions are seldom as fast as the 2–3 $\mathrm{m\,s^{-1}}$ speed of the first vertical mode, so this can be discounted. Third, and more seriously, depth-varying ocean motions are as fast as the few centimeters per second speed of the fastest baroclinic Rossby wave. A background flow – produced geostrophically by density variations across the ocean basin – can strongly modify the northward potential vorticity gradient of the system. Direct calculations of the changes this produces in phase speed suggest that much, but not all, of the discrepancy between observations and linear theory is explained by the presence of such background flows.

Conclusions

The ocean appears to possess Rossby waves in most of its basins. Theory for such waves has existed for many years, but they have only recently been observed by satellite altimeters and other approaches. The theory gives predictions of the right order of magnitude for Rossby wave speeds, but at mid and high latitudes appears to underestimate the speeds by a factor of 2. Various theories have been put forward to explain this discrepancy, of which the most promising is the inclusion of background mean flow, not as a simple depth-independent advection but as a genuine interaction with the wave. None of these theories forms a complete explanation. It will probably be necessary to combine the processes (e.g., to include both topographic variation and a background mean flow) before the theory can be regarded as satisfactory.

Symbols

a	Rossby, or deformation, radius
c_x, c_y	Phase velocity
c_{gx}, c_{gy}	Group velocity
f	Coriolis parameter
g	Acceleration due to gravity
h	Perturbation to depth of a fluid layer
k	Eastward wavenumber
l	Northward wavenumber
p	Pressure
t	Time
u	Eastward velocity
v	Northward velocity
w	Vertical velocity
x	Eastward coordinate
y	Northward coordinate
z	Vertical coordinate
C	Modal wave speed
H	Ocean depth, or equivalent depth
K	Modulus of wavenumber
N	Buoyancy frequency of water
β	Rate of change of f with distance north
ρ_0	Mean density of sea water
ω	Frequency

See also

Coastal Trapped Waves. Ekman Transport And Pumping. Internal Waves. Mesoscale Eddies. Wind Driven Circulation.

Further Reading

Chelton DB and Schlax MG (1996) Global observations of oceanic Rossby waves. *Science* 272: 234–238.

Dickinson RE (1978) Rossby waves — long-period oscillations of oceans and atmospheres. *Annual Reviews of Fluid Mechanics* 10: 159–195.

Gill AE (1982) *Atmosphere–Ocean Dynamics*. New York: Academic Press.

LeBlond PH and Mysak LA (1978) *Waves in the Ocean*. Amsterdam: Elsevier.

Rhines PB (1977) The dynamics of unsteady currents. In: Goldberg EG, McCave IN, O'Brien JJ and Steele JH (eds) *The Sea*, pp. 189–378. New York: Wiley.